

Simulation study investigating the role of vessel topology in differentiating normal and tumor vessels using transverse relaxation times

Mohammed Salman Shazeeb¹ and Bashar Issa¹

¹Department of Physics, UAE University, Al-Ain, Abu Dhabi, United Arab Emirates

Introduction: When simulating blood oxygenation level dependent (BOLD) contrast effects in functional magnetic resonance imaging (fMRI), most researchers make the general assumption that the brain vasculature is represented as 2D or 3D infinite long cylinders to simulate BOLD signal changes [1]. A more realistic model of the human cortical vasculature is more complicated with the vessels exhibiting branching, coiling, and forming different types of networks especially in tumor regions [2,3]. Tumorous tissue exhibit vessels with increased tortuosity and bifurcations with a larger diameter compared to that of normal tissue [3]. This study presents an alternate capillary model design to reflect a more realistic cortical vasculature in the brain for comparing vessels in normal and tumor tissues. Contrary to the conventional infinite cylinder design, we propose a cylinder fork design that captures the essence of curvature and tortuosity of vessels. Here, we attempt to quantitate the topology of the fork cylinder using the bifurcation angle β (Fig. 1b) and investigate its effect on MRI parameters. We predict that the bifurcation angle can be used to quantitate the state of the capillary vessels as either being from normal or tumor tissue.

Methods: Monte Carlo methods were used to quantify R2 and R2* for cylindrical fork perturbors at different bifurcation β angles. We modeled the vasculature using a cylinder fork model (CFM) composed of straight trunk (prior to bifurcation) of half cube length and the bifurcating segments. The cube is of 80 μm sides and incorporates cylinder fork segments ($n = 1, 3, 5, 7$ and 9) with varying β angles ($\beta = 0^\circ, 15^\circ, 30^\circ, 45^\circ, 60^\circ, 75^\circ, 90^\circ$) that were arranged close to symmetry without any overlapping vessels. For all the orientations and with multiple forks in the same cube, the cylinder trunks were set in a parallel orientation. The angle θ (Fig. 1a) between the trunk and the magnetic field was 90° for orientations 1 and 3 with the vessel lying in the xy-plane (Fig. 1c), while $\theta = 0^\circ$ for orientation 2. This model was converted into a cubic $128 \times 128 \times 128$ matrix with each cylinder element assigned a susceptibility value of 3×10^{-8} (cgs units). Magnetic field perturbations were calculated using a forward 3D Fourier transform of the susceptibility distribution of the CFM [4] which allows faster computation of the field variations. Signal generation was initiated by placing a proton at a random location outside the vessels to simulate extravascular signal. Each proton took 50 steps between a pair of 90° and 180° pulses distributed using a Gaussian model with zero mean and $\sigma = \sqrt{2 \cdot D \cdot \Delta t}$, where D is the diffusion constant set at $1 \times 10^{-9} \text{ m}^2/\text{s}$ and each time step $\Delta t = 0.2 \text{ ms}$. The random walk of the 20,000 protons was maintained outside the vessels assuming impermeability of the CFM. The phase accumulated by each proton during every step was calculated as $\gamma \cdot \Delta B \cdot \Delta t$ where γ is the gyromagnetic ratio and ΔB is the calculated magnetic field from the susceptibility map. The simulation was performed at true vessel diameters of 5 μm and 2.5 μm . R2 and R2* were calculated by linear least-square fitting of log signal intensity versus volume fraction. The R-squared values of all fittings were very high (~ 0.9). The use of relaxation rates per volume fraction unit will remove the dependence on vessel lengths and therefore emphasize the role of the bifurcation angle. Analysis of variance (ANOVA) test was performed to check for any significant effect of β on the relaxation times at different vessel diameters.

Results and Discussion: For all the orientations, R2 and R2* show a clear dependence on the bifurcation angle β but with different behavior depending on the orientation. ANOVA test showed a significant effect of β on R2 ($p < 0.01$) and R2* ($p < 0.03$) at the smaller diameter for all orientations while the effects were not significant at the larger diameter. In orientation 2, the maximum values of R2 and R2* occur at 90° for vessels at both diameters. With the smaller vessel diameter, both R2 and R2* behave with a W-profile with the values dipping from 0° and rising to 45° , and then dipping slightly at 60° before reaching a maximum at 90° (Figs. 2a & 2c). At the larger vessel diameter, R2* stays fairly constant between 0° and 45° ; between 60° and 90° , R2* increases in a linear fashion (Fig. 2d). R2, on the other hand, shows a concave upward profile with respect to β with the minimum occurring at 45° (Fig. 2b). The concavity is slightly skewed with the maximum R2* occurring at 90° . At 90° , the vessel has a T-shape in orientation 2 which presents the maximum disturbance in the local field caused by the interaction of B_0 and vessel geometry. The symmetry of R2 and R2* around 45° at the lower diameter only indicates that saturation of relaxation due to high susceptibility (i.e. large diameter) is not reached at this small diameter and diffusion is still effective. In orientations 1 and 3 at the smaller vessel diameter, a W-profile is observed for both R2 and R2* with respect to β (Fig. 2a & 2c) as noted with orientation 2. At the larger vessel diameter, a V-profile is more evident for R2 and R2* in both orientations (Fig. 2b & 2d). As before, it seems that the larger magnetic field deviations caused by the larger vessel diameter tend to dampen small variations in relaxation rates. In general, R2 and R2* values are highest for orientation 1 and lowest for orientation 2 except at the relatively larger β values.

Conclusion: R2 and R2* measurements indicate a clear dependence on the bifurcation angle β at different vessel diameters. Our simple CFM looks at the capillaries as parallel cylinders with bifurcation forks. We predict that in a tumor, the number of vessels and vessel diameters will be larger per voxel which might allow MRI parameters to clearly delineate normal versus tumor vessels. However, this model has to be further developed to incorporate a more realistic vascular network that would include other shapes like the loop vessel model (Fig. 1d). Ongoing work will further develop the vascular model to include cylinders at random orientations with different values of θ and ϕ (Fig. 1a) to create a more realistic scenario of the cortical vasculature, and to include intravascular signal. Abstract#4749 has been submitted which investigates the effect of the diffusion constant D on R2 and R2* relationship with the bifurcation angle.

References: [1] Marques and Bowtell (2008). *NMR Biomed* 21:553-565; [2] Duvernoy *et al.* (1981). *Brain Res Bull* 7:519-579; [3] Coomber *et al.* (1988). *J Neuropath Exp Neur* 47:29-40; [4] Marques and Bowtell (2005). *Concept Magn Reson B* 25B:65-78.

Acknowledgments: This work was funded by UAE-NRF Grant 31S087.

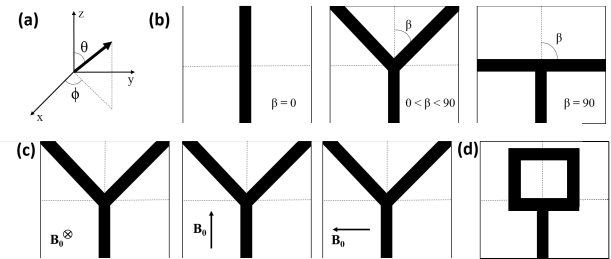


Fig. 1 – (a) Axis orientation depicting angles θ and ϕ . (b) Depiction of fork cylinders with different bifurcation angles β . (c) Orientation of the cylinder fork (shown here at $0^\circ < \beta < 90^\circ$) with respect to the magnetic field B_0 shown in three different directions: into the page (orientation 1), up (orientation 2), and to the left (orientation 3) of the Y-shape cross-section. (d) Depiction of the loop vessel model.

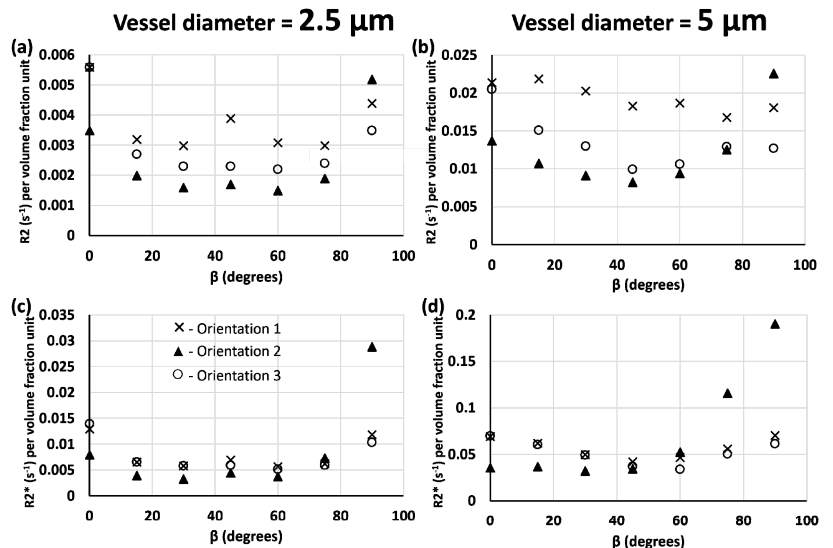


Fig. 2 – Plots showing dependence of R2 and R2* per volume fraction unit with respect to β in the three different orientations at different vessel diameters.